Journal of
Composites Science

MDPI

Article

Improving Mechanical, Thermal and Damping Properties of NiTi (Nitinol) Reinforced Aluminum Nanocomposites

Penchal Reddy Matli [1], Vyasaraj Manakari [1], Gururaj Parande [1], Manohar Reddy Mattli [2], Rana Abdul Shakoor [2] and Manoj Gupta [1,*]

[1] Department of Mechanical Engineering, National University of Singapore, Singapore 119077, Singapore; drlpenchal@gmail.com (P.R.M.); mbvyasaraj@u.nus.edu (V.M.); gururaj.parande@u.nus.edu (G.P.)
[2] Center for Advanced Materials, Qatar University, Doha 2713, Qatar; manoharreddy892@gmail.com (M.R.M.); shakoor@qu.edu.qa (R.A.S.)
* Correspondence: mpegm@nus.edu.sg; Tel.: +65-651-663-58

Received: 23 December 2019; Accepted: 13 February 2020; Published: 15 February 2020

Abstract: In the present study, $Ni_{50}Ti_{50}$ (NiTi) particle reinforced aluminum nanocomposites were fabricated using microwave sintering and subsequently hot extrusion. The effect of NiTi (0, 0.5, 1.0, and 1.5 vol %) content on the microstructural, mechanical, thermal, and damping properties of the extruded Al-NiTi nanocomposites was studied. Compared to the unreinforced aluminum, hardness, ultimate compression/tensile strength and yield strength increased by 105%, 46%, 45%, and 41% while elongation and coefficient of thermal expansion (CTE) decreased by 49% and 22%, respectively. The fabricated Al-1.5 NiTi nanocomposite exhibited significantly higher damping capacity (3.23×10^{-4}) and elastic modulus (78.48 ± 0.008 GPa) when compared to pure Al.

Keywords: nanocomposites; microwaves; extrusion; thermal analysis; damping behavior; mechanical properties

1. Introduction

Aluminum (Al) and its alloys have long been the preferred choice in weight critical applications in the defense, automotive, sports, and aerospace sectors owing to their exceptional physical, mechanical, and thermal properties such as lightweight, low cost, high specific strength, high specific modulus, and low coefficient of thermal expansion [1]. Particle reinforced aluminum metal matrix composites (AMMCs) have been extensively researched in the past two decades in view of replacing monolithic aluminum alloys to realize enhanced durability [2–8]. Ceramic materials such as SiC, Al_2O_3, BN, and TiC amongst others are often used as the reinforcement phases for developing Al-based composites [9–12]. In the recent times, the lightweight materials research community's emphasis has been to examine the effect of nano-sized reinforcement particle addition on the thermal and mechanical behavior of aluminum composites [10,13,14]. Also, metallic glasses as reinforcing phases have garnered considerable attention owing to their high hardness, mechanical strength, enhanced corrosion resistance, and good functionality [15–17]. Several researchers have reported that uniformly distributed metallic glass reinforcement nanoparticles have the ability to simultaneously improve the strength and ductility of AMMCs [2,18–21]. Hence, using metallic glass as a reinforcing phase in developing aluminum matrix nanocomposites [22–24] can be a viable option to improve the light-weighting capabilities in the aerospace and automotive industries.

$Ni_{50}Ti_{50}$ (Nitinol) alloy has great potential as reinforcement due to its high damping capacity, super-elastic, thermal, and mechanical properties [25]. Previous studies have shown the outstanding

improvements in mechanical properties of NiTi alloy reinforced Al [26–28], Mg [25,29], and Ag [30] matrix composites. Currently, NiTi alloy reinforced Al matrix composites have been fabricated primarily by friction stir processing, ultrasonic additive manufacturing, pressure infiltration process, and spark plasma sintering [26,28,31,32]. Among different synthesis methods used for Al-based composites, powder metallurgy using hybrid microwave sintering technique (MWS), is particularly suitable for the synthesis of composite materials as it provides excellent control over the particle size growth, microstructural changes, and volume fraction of matrix and reinforcement [33,34]. Reddy et al. successfully synthesized Al-based nanocomposites using Al_2O_3, TiC, Si_3N_4, B_4C, BN, and SiC reinforcements through the unique powder metallurgy technique coupled with hybrid microwave sintering. The presence of the secondary phases in the Al-matrix leads to progressive improvements in the mechanical and thermal properties of aluminum thereby highlighting the effectiveness of this technique to develop high-performance, lightweight, Al-based composites.

The studies on the influence of NiTi alloy particles on the Al matrix is still at an infancy stage. Furuya et al. [27] reported that 9 vol % NiTi incorporated Al matrix composites exhibited an ultimate compressive strength of 78 MPa and a yield strength of 62 MPa which is 105% and 77% improvement, respectively compared to Al. Hu et al. [31] discovered that an ultimate tensile strength (UTS) of 268 MPa was achieved at 1 h oxidized NiTi/Al composites via pressure infiltration process which was close to the theoretical value of 272 MPa at room temperature. Park et al. [35] synthesized NiTi/Al6061 composite material containing various percentages of NiTi reinforcement particles in the Al-6061 matrix showing significant improvement in tensile strength of up to 2 times with the presence of NiTi particles.

To the best of our knowledge, no report has been published so far which investigates the thermal, mechanical, and damping behavior of the Al-NiTi nanocomposites fabricated through powder metallurgy coupled with microwave sintering method. Therefore, the primary aim of the present work is to investigate the suitability of using the microwave sintering followed by hot extrusion technique to synthesize $Ni_{50}Ti_{50}$ containing Al nanocomposites and to study their microstructural evolution, mechanical, thermal, and damping properties.

2. Experimental Procedure

2.1. Materials Processing

Commercially available aluminum (Al) powder of size ~45 µm and a purity of >99.7% supplied by Merck (Darmstadt, Germany) was used as the matrix material, and $Ni_{50}Ti_{50}$ alloy nanoparticles having an average size of ~30–50 nm and purity >99% was procured from Nanostructured and Amorphous Materials, Inc. (Houston, TX, USA) were used as reinforcement element to produce Al-NiTi nanocomposites.

To produce Al-NiTi nanocomposites, NiTi alloy powder and pure Al were weighed carefully and blended at 200 rpm for 2 h using planetary ball mill (Retsch PM400, Haan, Germany). The blended powder was then compacted into cylindrical billets of 40 mm length and 35 mm diameter using a pressure of 97 bars (50 tons). The compacted billets were then sintered using microwave sintering at 550 °C under ambient conditions. Billets of microwave sintered Al and Al nanocomposites were homogenized at 400 °C for 1 h prior to hot extrusion at a temperature of 350 °C at an extrusion ratio of 20.25:1 on a 150-ton hydraulic press producing rods of 8 mm in diameter. Extruded rods were further used to prepare samples for different characterization studies.

2.2. Materials Characterization

X-ray diffraction (XRD) analysis of the Al nanocomposite samples was performed by a Shimadzu LAB-X XRD-6000 (Shimadzu Corporation, Osaka, Japan) using 0.1542 nm CuK_α radiation. Microstructural characterization of the extruded pure Al and Al-NiTi nanocomposites was carried out by using field emission scanning electron microscopy (FESEM-S4300, HITACHI LTD., Tokyo, Japan).

Microhardness of the Al-NiTi nanocomposite samples was measured by Vickers hardness tester (Matsuzawa MXT 50 and Shimadzu-HMV) at a load of 25 gf for a dwell time of 15 s. The nanohardness of the extruded Al-NiTi nanocomposites were examined using a MFP-3D NanoIndenter system.

Compressive and tensile tests were conducted on pure aluminum and nanocomposite samples according to ASTM E9-89a and ASTM E8/E8M-15a, respectively using Lloyd universal testing machine (LR 50 kN). For tensile tests, round samples of 5-mm diameter and 25-mm gauge length were used. The crosshead speed was set at 0.254 mm/min for 0.010 min^{-1} strain rate. For compression test, the samples of 8-mm length (l) and 8-mm diameter (d) where l/d = 1 were subjected to compression load at 0.005 min^{-1} strain rate using the crosshead speed of 0.04 mm/min. For each composition, a minimum of five tests were conducted to obtain repeatable values. A scanning electron microscope (Hitachi S-4300) was used to analyze fractured samples for determining the mode of failure under compression and tensile loading.

The coefficients of thermal expansion (CTE) of extruded aluminum and its composites was carried out in a thermomechanical analyzer (SETARAM 92-16/18). A heating rate of 5 °C/min was maintained with the flow rate of argon gas at 0.1 L per minute (lpm). With the aid of an alumina probe, the displacement experienced by the test samples was precision measured as a function of temperature.

The damping performance of the pure Al and Al-NiTi nanocomposites according to ASTM standard E1876-09 was analyzed using resonance frequency damping analyzer (RFDA, IMEC, Genk, Belgium). Each sample used for this study was 60 mm in length and 8 mm in diameter.

3. Results and Discussion

3.1. Microstructural Characterization

Figure 1a shows the XRD patterns of extruded Al-NiTi nanocomposites. The enlarged pattern for the Al-1.5 vol % NiTi nanocomposite is presented in Figure 1b. The existence of NiTi reinforcement phase in the Al matrix is evidently confirmed in the Al matrix. The X-ray patterns exhibit dominantly the peaks of aluminum at about 38° (111), 44° (200), 65° (220), 78° (311), and 83° (222) and very weak peaks of NiTi phase at about 42° (110) and 79° (211). These are the characteristic peaks and in agreement with the peaks observed by Czeppe et al. [36].

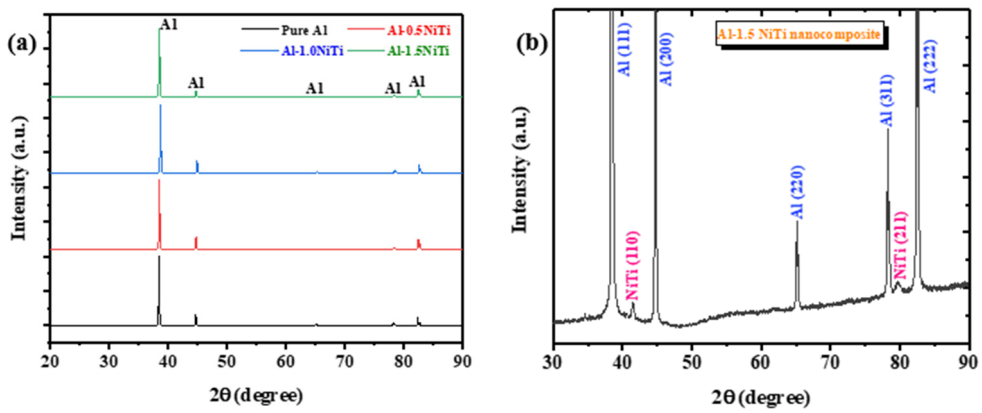

Figure 1. XRD spectra of the: (**a**) extruded Al-NiTi nanocomposites and (**b**) the enlarged XRD pattern of Al-1.5NiTi nanocomposite.

Figure 2a,b shows SEM micrographs of the pure Al and Al-NiTi nanocomposites with 1.5 vol % of NiTi. Figure 2b shows that NiTi particles are homogeneously distributed in the Al matrix. Besides the primary processing optimized parameters, the extrusion process also assisted in realizing good interfacial integrity between Al particles and NiTi nanoparticles and uniform distribution of NiTi particles.

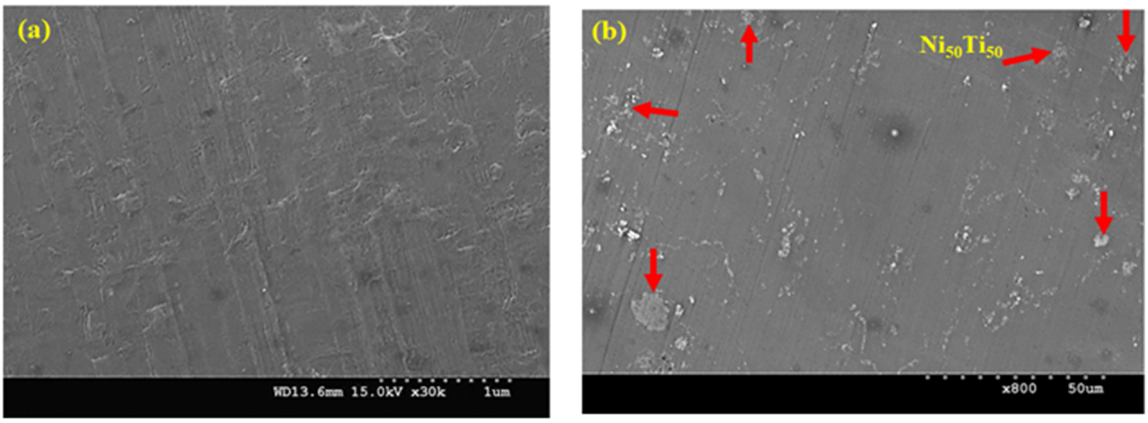

Figure 2. Representative SEM micrographs of: (**a**) pure Al and (**b**) Al-1.5NiTi nanocomposite.

3.2. Mechanical Properties

Microhardness, nanoindentation, and compression studies were conducted to assess the mechanical response of the developed nanocomposites. Figure 3a shows the microhardness values of Al-NiTi nanocomposites as a function of NiTi content. Progressive addition of NiTi (0–1.5 vol %) in the Al matrix improved the microhardness values from 38 ± 5 HV to 78 ± 5 HV. Figure 3b shows the nanoindentation response of Al and Al-NiTi nanocomposites. Nanohardness of the nanocomposites displayed a similar trend as the microhardness values. Nanohardness of pure Al also improved from 3.9 ± 0.22 GPa to 8.2 ± 0.4 GPa, with the addition of 1.5 vol % NiTi. The nanohardness data of Al-NiTi nanocomposites are also displayed in Table 1. Both the hardness tests, in common, revealed a significant increase in resistance to localized plastic deformation due to the increasing presence of NiTi nanoparticles in the Al matrix.

The presence of hard nano-NiTi particles (~600 Hv) improves the microhardness of the composites as explained by the rule of mixtures [37].

$$H_c = H_m F_m + H_r F_r \quad (1)$$

where, H_c, H_m, and H_r represents the hardness of the composite, matrix, and reinforcement, while F_r and F_m are the volume fraction of reinforcement and matrix, respectively.

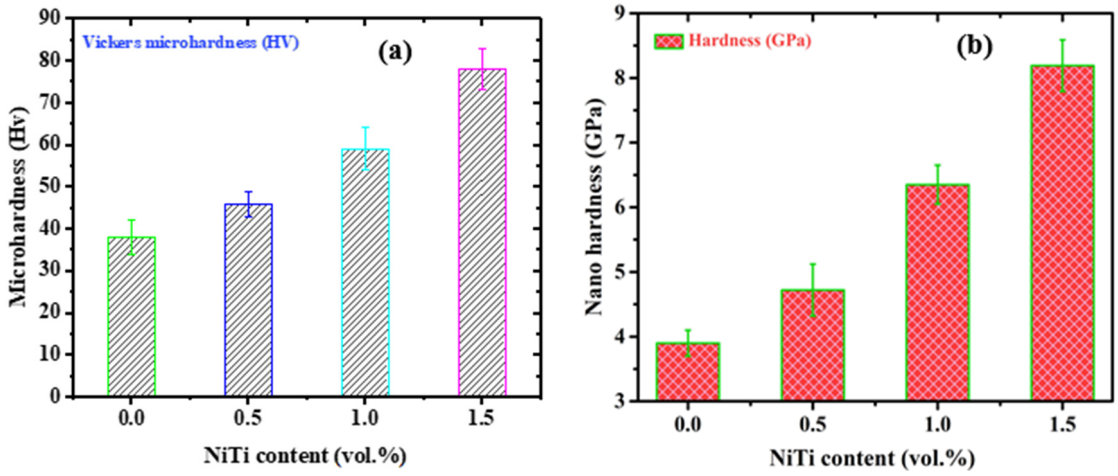

Figure 3. *Cont.*

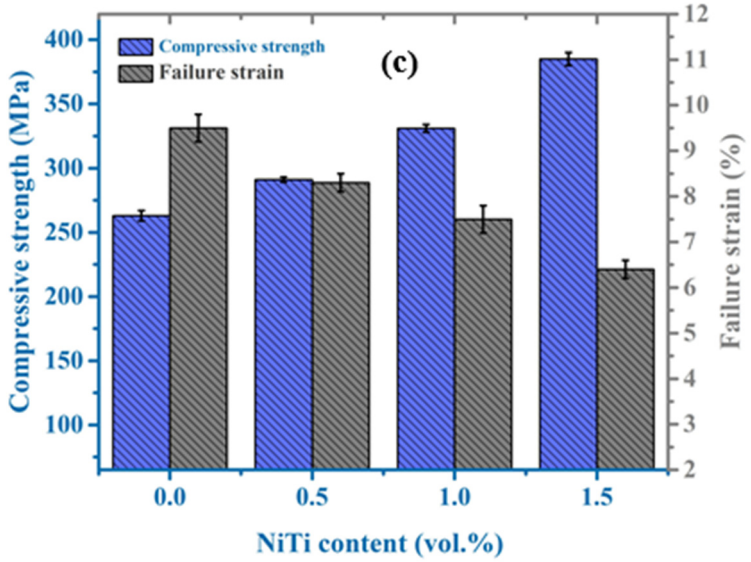

Figure 3. (**a**) Vickers microhardness, (**b**) nano hardness, and (**c**) compressive properties of extruded Al-NiTi nanocomposites as a function of NiTi content.

Table 1. Comparison of mechanical properties of Al–NiTi nanocomposites with other studies.

Sample	Hardness		Compressive Properties			Tensile Properties		
	(Hv) Micro	(GPa) Nano	CYS (MPa)	UCS (MPa)	Failure Strain (%)	TYS (MPa)	UTS (MPa)	Elongation (%)
Pure Al	38 ± 4	3.9 ± 0.2	70 ± 3	263 ± 4	9.5 ± 0.2	106 ± 3	119 ± 3	10.8 ± 0.5
Al-0.5 vol % NiTi	46 ± 3 (↑21%)	4.7 ± 0.4 (↑20%)	76 ± 2 (↑8%)	291 ± 2 (↑10%)	8.3 ± 0.4 (↓12%)	124 ± 5 (↑17%)	136 ± 3 (↑14%)	9.2 ± 0.2 (↓15%)
Al-1.0 vol % NiTi	59 ± 5 (↑55%)	6.3 ± 0.3 (↑61%)	88 ± 3 (↑25%)	331 ± 3 (↑26%)	7.5 ± 0.3 (↓21%)	141 ± 2 (↑33%)	152 ± 4 (↑28%)	7.8 ± 0.4 (↓28%)
Al-1.5 vol % NiTi	78 ± 5 (↑105%)	8.2 ± 0.4 (↑110%)	97 ± 4 (↑38%)	385 ± 5 (↑46%)	6.4 ± 0.4 (↓32%)	154 ± 3 (↑45%)	168 ± 5 (↑41%)	5.5 ± 0.2 (↓49%)
Al-5 vol % $Ni_{60}Nb_{60}$ [2]	74.5 ± 4	–	114 ± 6	300 ± 5	>50	50 ± 9	60 ± 3	16.8 ± 2
Al-1.5 vol % BN [10]	88 ± 4	9.5 ± 0.5	64 ± 6	391 ± 5	6.3 ± 0.3	144 ± 2	158 ± 4	6.9 ± 0.4
Al-1.5 vol % SiC [11]	82 ± 4	–	114 ± 7	392 ± 6	>75	158 ± 9	178 ± 6	7.3 ± 0.9
Al-4 vol % $Ni_{49.8}Nb_{50.2}$ [27]	–	–	–	–	–	32	38	>4
Al-3 wt % SiO_2 [38]	38.7	–	142	268	2.8	100	137	0.9
Al-4 vol % (Ti,W)C [39]	52 ± 4	–	118 ± 1	346 ± 6	39 ± 2	–	–	–

Room temperature compressive properties of extruded Al-NiTi nanocomposites are summarized in Figure 3c and Table 1. It is found that with the increasing amount of nano-NiTi alloy particles the compressive yield strength (CYS) and ultimate compression strength (UCS) showed a significant increase from 70 ± 3 MPa to 97 ± 4 MPa and 263 ± 4 MPa to 385 ± 5 MPa, respectively. Correspondingly, the ductility of the composites showed a decline. The average yield strength and ultimate compressive strength of extruded pure Al and Al-NiTi nanocomposites are listed in Table 1. It can be observed that the addition of 1.5 vol % NiTi into the Al matrix, the compressive strength and yield strength of the composites increased by 46.4% and 38.5% compared with Al. A substantial increase in the compression strength of the Al-matrix material is attributed to the addition of the nano-NiTi reinforcement phase.

The stress–strain curves and the mechanical data of Al-NiTi nanocomposites (0–1.5 vol %) under tensile loads are illustrated in Figure 4a,b. The incorporation of NiTi nanoparticles into pure Al matrix led to progressive improvement in tensile yield strength (TYS) and ultimate tensile strength (UTS), from 106 ± 3 MPa to 154 ± 4 MPa, and from 119 ± 3 MPa to 168 ± 5 MPa, with the percentage of elongation decreasing from 10.8% to 5.5%. The data of yield strength, ultimate tensile strength (UTS), and elongation (%) of the synthesized Al-matrix composites are presented in Table 1.

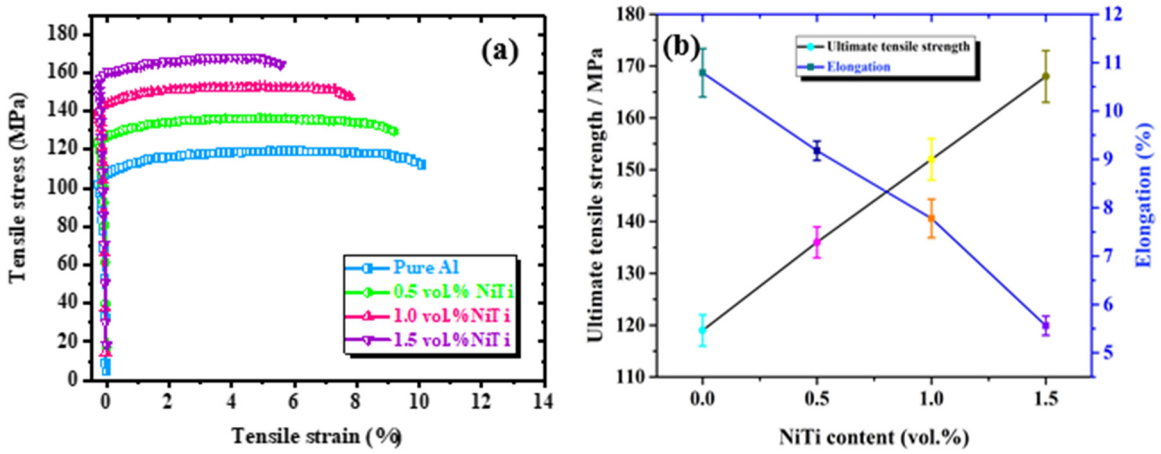

Figure 4. (**a**) Typical tensile stress–strain curves and (**b**) ultimate tensile strength and ductility for pure Al and Al-NiTi nanocomposites.

On incorporating 1.5 vol % NiTi particles to the Al matrix, the tensile strength and yield strength of the NiTi particle reinforced composites increased by 41.14% and 45.3% compared with that of Al, respectively. In addition, the mechanical properties of the Al-NiTi nanocomposites are compared with the recently published Al-based composites as listed in Table 1 [27]. It can also be observed the Al-NiTi nanocomposites superior/comparable with other Al-based nanocomposites [2,10,11,38,39].

Factors contributing to the strength improvement could be the Orowan strengthening mechanism and increase in dislocation density due to CTE and elastic modulus differences between pure Al and NiTi nanoparticles. The tensile failure strain showed a decreasing trend with the progressive addition of NiTi nanoparticles. The tensile elongation decreases (~49%) with increasing NiTi content. The presence of hard NiTi nanoparticles tends to the formation of cracks and subsequent debonding leading to reduction in ductility. However, the fracture strain values exhibited by the composites is still significant from a deformation perspective (>5%) [9].

Possible Strengthening Mechanisms

The enhancement of mechanical properties in the extruded composite material could be attributed to the following reasons: (a) presence of fairly dispersed NiTi particles leading to Orowan strengthening; (b) mismatch in coefficient of thermal expansion and elastic modulus values leading to dislocation generations; and (c) effective transferring of load from the soft Al matrix to the hard NiTi nanoparticles due to good interfacial bonding.

Orowan strengthening is a result of the resistance offered by ultrafine hard particulates to the dislocation movement [40]. The Orowan loop mechanism forms dislocation loops around the NiTi nanoparticles leading to work hardening effects and contributes to strengthening of Al-NiTi nanocomposites. According to Orowan mechanism, the uniform distribution of hard phase NiTi nanoparticles in Al matrix results in higher strength as per equation (2) [41,42]

$$\Delta_\sigma = \phi G_m b / \lambda \quad (2)$$

where λ is the interparticle spacing, b is Burgers vector, G_m is the shear modulus of the matrix, and φ is a constant.

The thermal mismatch in composites is generally related to the difference in thermal expansion coefficients between matrix and reinforcement phases. The CTE values of the Al matrix and nano-NiTi particles are 23.31 μ/K and 10 μ/K, respectively [41]. The CTE mismatch between Al and NiTi induces plastic residual stress, increasing the dislocation density and the strength of composites. This strengthening is predicted using the following equation (3) [24]

$$\rho = \frac{B\varepsilon V_r}{bd(1-V_r)} \tag{3}$$

where B is a geometric constant, V_r is the volume fraction of the particles, ε is the difference in CTE between Al matrix and the NiTi particles, b is the Burgers vector of the matrix, and d is the average grain diameter of reinforcements.

3.3. Fracture Behavior

Fractured images of compression and tension test failed pure Al and Al-1.5 NiTi nanocomposite samples are shown in Figure 5. Typical shear band formations are observed (Figure 5a,c), which is consistent with the observations made by other researchers on Al-based nanocomposites [9–11]. Tensile fractography (Figure 5b,d) shows the dimple shaped features indicating a ductile fracture.

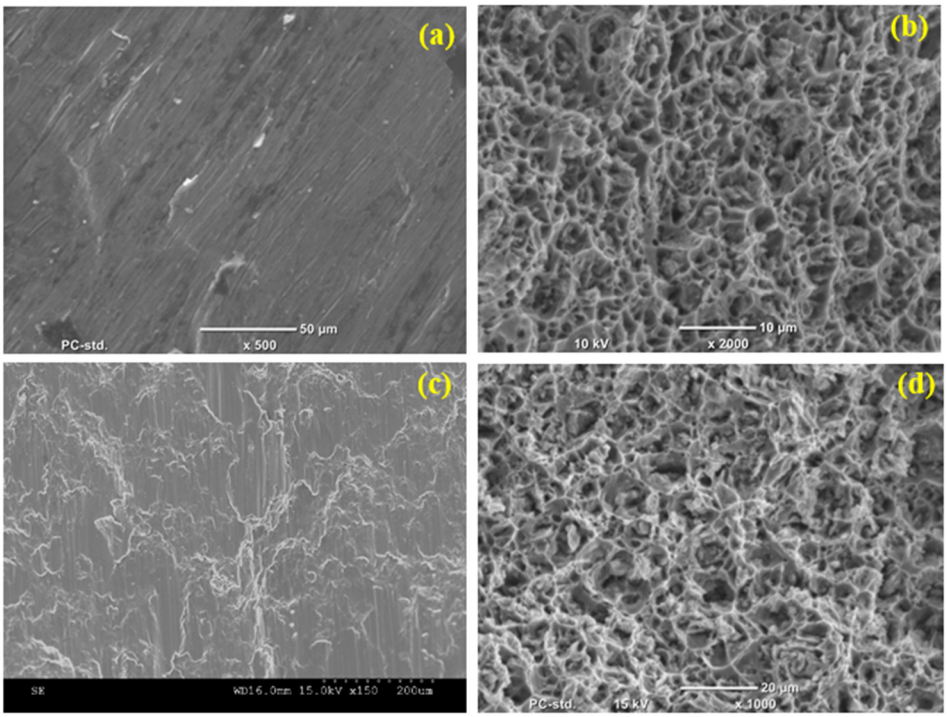

Figure 5. Compression (**a**,**c**) and tensile (**b**,**d**) fractography images of pure Al and Al-1.5 NiTi nanocomposite.

3.4. Coefficient of Thermal Expansion

The dimensional stability of the composite is reflected by its CTE. The coefficient of thermal expansion (CTE) behavior of extruded aluminum nanocomposites containing nano-NiTi alloy particles is shown in Figure 6.

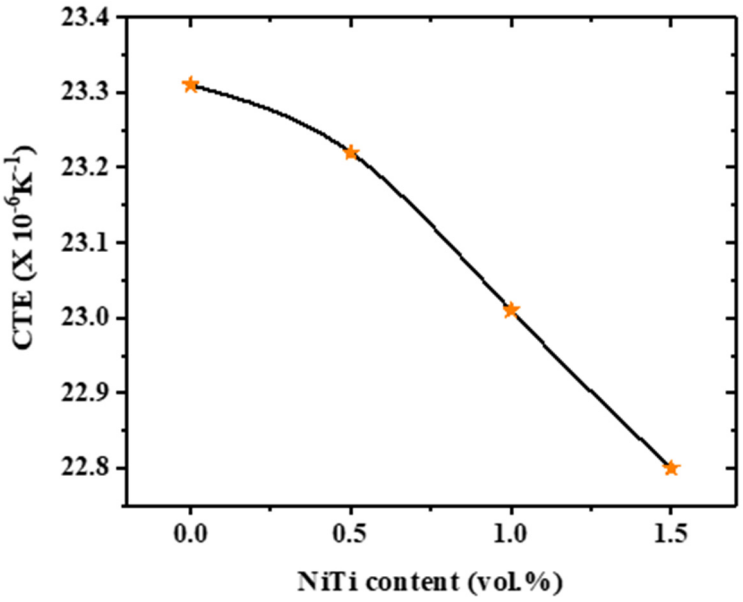

Figure 6. Effect of NiTi content on the coefficient of thermal expansion (CTE).

The CTE values for Al-0.5 vol % NiTi (23.22 μ/K), Al-1.0 vol % NiTi (23.01 μ/K) and Al-1.5 vol % NiTi (22.8 μ/K) were found to be ~3.8%, ~12.8%, and ~21.8% lower than that of pure Al (23.31 μ/K). This considerable decrement in CTE is attributed to the addition of thermally stable nano-NiTi alloy particles having lower CTE of 10 μ/K [41]. Also, the lower CTE of the composites can be attributed to a reasonably uniform distribution of particles within the matrix which is evident from the microstructural examinations. To note that improvement in the thermal and dimensional stability is key in activating the Forest strengthening mechanism leading to the strengthening of the nanocomposites [37].

3.5. Damping Behavior

Vibration damping capabilities of pure Al and Al-1.5 NiTi nanocomposite are displayed in Figure 7 and Table 2. An enhancement in the damping capacity (Q^{-1}) and the damping loss rate (L) of pure Al is observed with the incorporation of NiTi nanoparticles greater/equal to one volume percent. In this investigation, optimum values of damping capacity and damping loss rate at ~6.15 and ~17.15×10^{-4}, respectively were achieved for Al-1.5 NiTi nanocomposite. The damping capacity and damping loss rate for the nanocomposite sample improved by ~15.4% and ~16.2% when compared to that of pure Al, respectively.

With the addition of 0.5 vol % NiTi nanoparticles, damping capacity of pure Al is decreased initially as the movements of dislocations in the composites are hindered by the NiTi reinforcements [43]. However, enhancement in the damping properties of nanocomposites with increasing addition of NiTi nanoparticles can be attributed to several damping mechanisms such as the presence of a plastic zone around reinforcement, increase in dislocation density, and due to other damping sources, such as grain boundary sliding mechanisms, defects, and porosities [44,45]. The damping capacities of the nanocomposites developed are resultant of the competing interactions between these contributing factors [46]. The CTE of NiTi and Al is 10 and 23.31×10^{-6}/K respectively. This difference of thermal expansion coefficient between Al and NiTi might induce high residual stresses around the particulates in the Al matrix, resulting in the formation of plastic deformation zone at the particle/matrix interface. According to the plastic zone damping model proposed Carreno-Morelli et al. [47], damping capacity of a material depends directly on the volume fraction of plastic zone. Therefore, progressive increase in the energy dissipation of Al-NiTi nanocomposites can be attributed to the higher amount of plastic zone around NiTi nanoparticles and further, at higher volume fractions, effects are multifold resulting to such

a rise in damping capacity of nanocomposites. Furthermore, significantly higher damping capacities realized for Al-1.0 vol % NiTi and Al-1.5 vol % NiTi nanocomposites can be due to overlapping of plastic zones, caused when the plastic zone is larger compared to smaller inter-particulate distances as the volume fraction of nanoparticle increases. This increase in the presence of plastic zones due to the presence of NiTi nanoparticles leading to an increase in the hardness of the nanocomposite samples is found to be substantially high when compared to pure Al. Furthermore, from Table 2, it can be observed that the elastic modulus of the nanocomposite sample increases with the addition of the NiTi nanoparticles. This is consistent with the trend exhibited by the Al-based metal matrix composite [10].

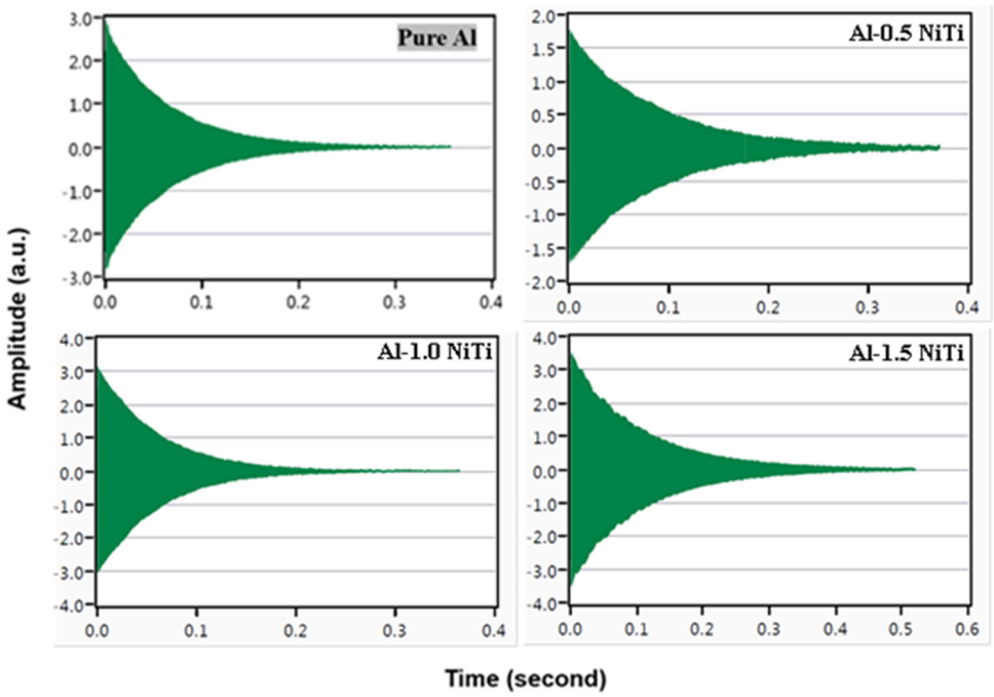

Figure 7. Damping characteristics of pure Al and Al (0.5, 1, and 1.5 vol %) NiTi nanocomposites.

Table 2. Elastic modulus and damping characteristics of extruded Al-NiTi nanocomposites.

Composition	Damping Capacity ($\times 10^{-4}$)	Damping Loss Rate	Elastic Modulus (GPa)
Pure Al	5.33 ± 0.056	14.76 ± 0.09	71.65 ± 0.02
Al-0.5 vol % NiTi	4.17 ± 0.031 (↓21.7%)	11.65 ± 0.06 (↓21%)	75.99 ± 0.02 (↑6.05%)
Al-1.0 vol % NiTi	5.65 ± 0.029 (↑6%)	15.2 ± 0.06 (↑2.98%)	76.48 ± 0.01 (↑6.74%)
Al-1.5 vol % NiTi	6.15 ± 0.029 (↑15.4%)	17.15 ± 0.06 (↑16.19%)	75.93 ± 0.08 (↑5.97%)

4. Conclusions

In this study, Al-NiTi nanocomposites were fabricated using hybrid microwave sintering followed by hot extrusion. The microstructural, mechanical, thermal, and damping performance were investigated. SEM results indicate that nano-NiTi alloy particles are homogeneously distributed in the Al matrix. Nanohardness of nanocomposites increased from 3.9 ± 0.2 GPa for pure Al to 8.2 ± 0.4 GPa for Al-1.5 NiTi nanocomposite. Compression tests revealed an increase in the strength from 263 ± 4 MPa for pure Al to 385 ± 5 MPa (~46%) for Al-1.5 NiTi nanocomposite. By increasing the reinforcement content up to 1.5 vol %, tensile strength of the samples was improved from 119 ± 3 MPa for pure Al to 168±5 MPa (~41%) for Al-1.5 NiTi nanocomposite. The enhanced mechanical properties

are attributed to the secondary processing, homogenously distributed particles, good Al/NiTi interfacial integrity, and dispersion strengthening. The coefficient of thermal expansion showed a reverse trend indicating an increase in thermal stability. The Al-1.5 NiTi nanocomposite showed the best damping (damping loss rate, damping capacity, and elastic modulus) response. From the processing perspective, hybrid microwave sintering has a potentially wider range of advantages and potential in the preparation of Al-based nanocomposites tools because of the advantages associated with its rapid heating capability.

Author Contributions: Investigation and writing—original draft preparation, P.R.M.; Formal analysis, G.P., V.M., Writing—review and editing, M.R.M. and R.A.S.; Conceptualization and supervision, M.G. All authors have read and agreed to the published version of the manuscript.

Funding: This research received no external funding.

Conflicts of Interest: The authors declare no conflict of interest.

References

1. Reddy, M.P.; Manakari, V.; Parande, G.; Shakoor, R.; Srivatsan, T.; Gupta, M. The Mechanical and Thermal Response of Shape Memory Alloy-Reinforced Aluminum Nanocomposites. In *Nanocomposites VI: Nanoscience and Nanotechnology in Advanced Composites*; Springer: Berlin/Heidelberg, Germany, 2019; pp. 51–62.
2. Jayalakshmi, S.; Gupta, S.; Sankaranarayanan, S.; Sahu, S.; Gupta, M. Structural and mechanical properties of Ni60Nb40 amorphous alloy particle reinforced Al-based composites produced by microwave-assisted rapid sintering. *Mater. Sci. Eng. A* **2013**, *581*, 119–127. [CrossRef]
3. Koli, D.K.; Agnihotri, G.; Purohit, R. Advanced aluminium matrix composites: The critical need of automotive and aerospace engineering fields. *Mater. Today Proc.* **2015**, *2*, 3032–3041. [CrossRef]
4. Matli, P.R.; Ubaid, F.; Shakoor, R.A.; Parande, G.; Manakari, V.; Yusuf, M.; Mohamed, A.M.A.; Gupta, M. Improved properties of Al–Si 3 N 4 nanocomposites fabricated through a microwave sintering and hot extrusion process. *RSC Adv.* **2017**, *7*, 34401–34410. [CrossRef]
5. Miracle, D. Metal matrix composites–from science to technological significance. *Compos. Sci. Technol.* **2005**, *65*, 2526–2540. [CrossRef]
6. Torralba, J.D.; Da Costa, C.; Velasco, F. P/M aluminum matrix composites: An overview. *J. Mater. Process. Technol.* **2003**, *133*, 203–206. [CrossRef]
7. Zhang, Y.; Ma, N.; Wang, H.; Le, Y.; Li, X. Damping capacity of in situ TiB2 particulates reinforced aluminium composites with Ti addition. *Mater. Des.* **2007**, *28*, 628–632. [CrossRef]
8. Reddy, M.P.; Manakari, V.; Parande, G.; Shakoor, R.A.; Mohamed, A.M.A.; Gupta, M. Structural, mechanical and thermal characteristics of Al-Cu-Li particle reinforced Al-matrix composites synthesized by microwave sintering and hot extrusion. *Compos. Part B Eng.* **2019**, *164*, 485–492. [CrossRef]
9. Reddy, M.P.; Himyan, M.; Ubaid, F.; Shakoor, R.; Vyasaraj, M.; Gururaj, P.; Yusuf, M.; Mohamed, A.; Gupta, M. Enhancing thermal and mechanical response of aluminum using nanolength scale TiC ceramic reinforcement. *Ceram. Int.* **2018**, *44*, 9247–9254. [CrossRef]
10. Reddy, M.P.; Manakari, V.; Parande, G.; Ubaid, F.; Shakoor, R.; Mohamed, A.; Gupta, M. Enhancing compressive, tensile, thermal and damping response of pure Al using BN nanoparticles. *J. Alloys Compd.* **2018**, *762*, 398–408. [CrossRef]
11. Reddy, M.P.; Shakoor, R.; Parande, G.; Manakari, V.; Ubaid, F.; Mohamed, A.; Gupta, M. Enhanced performance of nano-sized SiC reinforced Al metal matrix nanocomposites synthesized through microwave sintering and hot extrusion techniques. *Prog. Nat. Sci. Mater. Int.* **2017**, *27*, 606–614. [CrossRef]
12. Reddy, M.P.; Ubaid, F.; Shakoor, R.; Parande, G.; Manakari, V.; Mohamed, A.; Gupta, M. Effect of reinforcement concentration on the properties of hot extruded Al-Al2O3 composites synthesized through microwave sintering process. *Mater. Sci. Eng. A* **2017**, *696*, 60–69. [CrossRef]
13. Moazami-Goudarzi, M.; Akhlaghi, F. Wear behavior of Al 5252 alloy reinforced with micrometric and nanometric SiC particles. *Tribol. Int.* **2016**, *102*, 28–37. [CrossRef]
14. Soltani, N.; Sadrnezhaad, S.; Bahrami, A. Manufacturing wear-resistant 10Ce-TZP/Al2O3 nanoparticle aluminum composite by powder metallurgy processing. *Mater. Manuf. Process.* **2014**, *29*, 1237–1244. [CrossRef]
15. Byrne, C.J.; Eldrup, M. Bulk metallic glasses. *Science* **2008**, *321*, 502–503. [CrossRef]

16. Manakari, V.; Parande, G.; Doddamani, M.; Gupta, M. Evaluation of wear resistance of magnesium/glass microballoon syntactic foams for engineering/biomedical applications. *Ceram. Int.* **2019**, *45*, 9302–9305. [CrossRef]
17. Manakari, V.; Parande, G.; Doddamani, M.; Gupta, M. Enhancing the ignition, hardness and compressive response of magnesium by reinforcing with hollow glass microballoons. *Materials* **2017**, *10*, 997. [CrossRef]
18. Reddy, M.P.; Ubaid, F.; Shakoor, R.; Mohamed, A. Microstructure and Mechanical Behavior of Microwave Sintered Cu 50 Ti 50 Amorphous Alloy Reinforced Al Metal Matrix Composites. *JOM* **2018**, *70*, 817–822. [CrossRef]
19. Scudino, S.; Liu, G.; Prashanth, K.; Bartusch, B.; Surreddi, K.; Murty, B.; Eckert, J. Mechanical properties of Al-based metal matrix composites reinforced with Zr-based glassy particles produced by powder metallurgy. *Acta Mater.* **2009**, *57*, 2029–2039. [CrossRef]
20. Scudino, S.; Surreddi, K.; Sager, S.; Sakaliyska, M.; Kim, J.; Löser, W.; Eckert, J. Production and mechanical properties of metallic glass-reinforced Al-based metal matrix composites. *J. Mater. Sci.* **2008**, *43*, 4518–4526. [CrossRef]
21. Wang, Z.; Tan, J.; Scudino, S.; Sun, B.; Qu, R.; He, J.; Prashanth, K.; Zhang, W.; Li, Y.; Eckert, J. Mechanical behavior of Al-based matrix composites reinforced with $Mg_{58}Cu_{28.5}Gd_{11}Ag_{2.5}$ metallic glasses. *Adv. Powder Technol.* **2014**, *25*, 635–639. [CrossRef]
22. Chau, E.; Friend, C.; Allen, D.; Hora, J.; Webster, J. A technical and economic appraisal of shape memory alloys for aerospace applications. *Mater. Sci. Eng. A* **2006**, *438*, 589–592. [CrossRef]
23. Huang, W. On the selection of shape memory alloys for actuators. *Mater. Des.* **2002**, *23*, 11–19. [CrossRef]
24. Meenashisundaram, G.; Nai, M.; Gupta, M. Effects of primary processing techniques and significance of hall-petch strengthening on the mechanical response of magnesium matrix composites containing TiO_2 nanoparticulates. *Nanomaterials* **2015**, *5*, 1256–1283. [CrossRef] [PubMed]
25. Parande, G.; Manakari, V.; Wakeel, S.; Kujur, M.; Gupta, M. Enhancing Mechanical Response of Monolithic Magnesium Using Nano-NiTi (Nitinol) Particles. *Metals* **2018**, *8*, 1014. [CrossRef]
26. Chen, X.; Hehr, A.; Dapino, M.J.; Anderson, P.M. Deformation mechanisms in NiTi-Al composites fabricated by ultrasonic additive manufacturing. *Shape Mem. Superelasticity* **2015**, *1*, 294–309. [CrossRef]
27. Furuya, Y.; Sasaki, A.; Taya, M. Enhanced mechanical properties of TiNi shape memory fiber/Al matrix composite. *Mater. Trans. JIM* **1993**, *34*, 224–227. [CrossRef]
28. Ni, D.; Wang, J.; Zhou, Z.; Ma, Z. Fabrication and mechanical properties of bulk NiTip/Al composites prepared by friction stir processing. *J. Alloys Compd.* **2014**, *586*, 368–374. [CrossRef]
29. Guo, W.; Kato, H. Development of a high-damping NiTi shape-memory-alloy-based composite. *Mater. Lett.* **2015**, *158*, 1–4. [CrossRef]
30. Hao, S.; Cui, L.; Jiang, J.; Guo, F.; Xiao, X.; Jiang, D.; Yu, C.; Chen, Z.; Zhou, H.; Wang, Y. A novel multifunctional NiTi/Ag hierarchical composite. *Sci. Rep.* **2014**, *4*, 5267. [CrossRef]
31. Hu, J.; Zhang, Q.; Wu, G.; Liu, Y.; Li, D. Effect of pre-oxidation of TiNi fibers on the interfacial and mechanical property of TiNif/Al composite. *Mater. Sci. Eng. A* **2014**, *597*, 20–28. [CrossRef]
32. Wang, Z.; Dong, P.; Wang, W.; Yan, Z.; Ding, M. Interface formation of TiNif/Al composites fabricated by spark plasma sintering. *J. Alloys Compd.* **2017**, *726*, 507–513. [CrossRef]
33. Sun, C.; Song, M.; Wang, Z.; He, Y. Effect of particle size on the microstructures and mechanical properties of SiC-reinforced pure aluminum composites. *J. Mater. Eng. Perform.* **2011**, *20*, 1606–1612. [CrossRef]
34. Thakur, S.K.; Tun, K.S.; Gupta, M. Enhancing uniform, nonuniform, and total failure strain of aluminum by using SiC at nanolength scale. *J. Eng. Mater. Technol.* **2010**, *132*, 041002. [CrossRef]
35. Park, Y.C.; Lee, G.C.; Furuya, Y. A study on the fabrication of TiNi/Al6061 shape memory composite material by hot-press method and its mechanical property. *Mater. Trans.* **2004**, *45*, 264–271. [CrossRef]
36. Czeppe, T.; Levintant-Zayonts, N.; Swiatek, Z.; Michalec, M.; Bonchyk, O.; Savitskij, G. Inhomogeneous structure of near-surface layers in the ion-implanted NiTi alloy. *Vacuum* **2009**, *83*, S214–S219. [CrossRef]
37. Ceschini, L.; Dahle, A.; Gupta, M.; Jarfors, A.E.W.; Jayalakshmi, S.; Morri, A.; Rotundo, F.; Toschi, S.; Singh, R.A. Mechanical Behavior of Al and Mg Based Nanocomposites. In *Aluminum and Magnesium Metal Matrix Nanocomposites*; Springer: Berlin/Heidelberg, Germany, 2017; pp. 95–137.
38. Issa, H.K.; Taherizadeh, A.; Maleki, A.; Ghaei, A. Development of an aluminum/amorphous nano-SiO_2 composite using powder metallurgy and hot extrusion processes. *Ceram. Int.* **2017**, *43*, 14582–14592. [CrossRef]

39. Zheng, R.; Wu, Y.; Liao, S.; Wang, W.; Wang, W.; Wang, A. Microstructure and mechanical properties of Al/(Ti, W) C composites prepared by microwave sintering. *J. Alloys Compd.* **2014**, *590*, 168–175. [CrossRef]
40. Parande, G.; Manakari, V.; Meenashisundaram, G.K.; Gupta, M. Enhancing the tensile and ignition response of monolithic magnesium by reinforcing with silica nanoparticulates. *J. Mater. Res.* **2017**, *32*, 2169–2178. [CrossRef]
41. Armstrong, W.D. A one-dimensional model of a shape memory alloy fiber reinforced aluminum metal matrix composite. *J. Intell. Mater. Syst. Struct.* **1996**, *7*, 448–454. [CrossRef]
42. Ashby, M. Second Bolton Landing Conference on Oxide Dispersion Strengthening. *Gordon Breach N. Y.* **1968**, 47.
43. Parande, G.; Manakari, V.; Meenashisundaram, G.K.; Gupta, M. Enhancing the hardness/compression/damping response of magnesium by reinforcing with biocompatible silica nanoparticulates. *Int. J. Mater. Res.* **2016**, *107*, 1091–1099. [CrossRef]
44. Kujur, M.S.; Manakari, V.; Parande, G.; Tun, K.S.; Mallick, A.; Gupta, M. Enhancement of thermal, mechanical, ignition and damping response of magnesium using nano-ceria particles. *Ceram. Int.* **2018**, *44*, 15035–15043. [CrossRef]
45. Kujur, M.S.; Mallick, A.; Manakari, V.; Parande, G.; Tun, K.S.; Gupta, M. Significantly enhancing the ignition/compression/damping response of monolithic magnesium by addition of Sm_2O_3 nanoparticles. *Metals* **2017**, *7*, 357. [CrossRef]
46. Parande, G.; Manakari, V.; Kopparthy, S.D.S.; Gupta, M. A study on the effect of low-cost eggshell reinforcement on the immersion, damping and mechanical properties of magnesium–zinc alloy. *Compos. Part B Eng.* **2020**, *182*, 107650. [CrossRef]
47. Carreno-Morelli, E.; Urreta, S.; Schaller, R. Mechanical spectroscopy of thermal stress relaxation at metal–ceramic interfaces in Aluminium-based composites. *Acta Mater.* **2000**, *48*, 4725–4733. [CrossRef]